



HAL
open science

SEFI Modeling in Readout Integrated Circuit Induced by Heavy Ions at Cryogenic Temperatures

Laurent Artola, Samuel Ducret, Frédéric Advent, Guillaume Hubert, Julien
Mekki

► **To cite this version:**

Laurent Artola, Samuel Ducret, Frédéric Advent, Guillaume Hubert, Julien Mekki. SEFI Modeling in Readout Integrated Circuit Induced by Heavy Ions at Cryogenic Temperatures. *IEEE Transactions on Nuclear Science*, 2019, 66 (1), pp.452 - 457. 10.1109/tns.2018.2880791 . hal-04788604

HAL Id: hal-04788604

<https://hal.science/hal-04788604v1>

Submitted on 18 Nov 2024

HAL is a multi-disciplinary open access archive for the deposit and dissemination of scientific research documents, whether they are published or not. The documents may come from teaching and research institutions in France or abroad, or from public or private research centers.

L'archive ouverte pluridisciplinaire **HAL**, est destinée au dépôt et à la diffusion de documents scientifiques de niveau recherche, publiés ou non, émanant des établissements d'enseignement et de recherche français ou étrangers, des laboratoires publics ou privés.

SEFI Modeling in Readout Integrated Circuit Induced by Heavy Ions at Cryogenic Temperatures

L. Artola¹, Senior Member, IEEE, S. Ducret, F. Advent, G. Hubert², and J. Mekki³, Member, IEEE

Abstract—This paper presents a modeling approach of single-event functional interrupt (SEFI) which takes into account all the physical and electrical processes from the radiation particle down to the event at the system level. This paper is focused on the evaluation of SEFI sensitivity by experimental and simulation analyses of a readout integrated circuit (ROIC) designed by Sofradir for their infrared image sensors. Relevant correlations between simulation and experimental results of SEFI cross sections for heavy ions are presented and discussed. The simulation results confirm the strong SEFI robustness of the ROIC at 57 K.

Index Terms—Heavy ions, infrared (IR) detectors, low temperatures, modeling, readout integrated circuit (ROIC), single-event functional interrupt (SEFI).

I. INTRODUCTION

THE space environment is known to be a harsh environment in terms of temperature, vibration, and radiation for embedded devices and circuits. Soft error (SE) can be induced in electronics systems by radiation particles [1], [2], such as cosmic rays, protons, and even electrons (more recently) [3].

The complementary metal–oxide–semiconductor (CMOS) technology is the main technology used in on-board systems, especially in digital circuits such as the readout integrated circuit (ROIC) of CMOS image sensors (CIS) or infrared (IR) image sensors. The pixel array is controlled by the readout circuit of the image sensor. A readout circuit is composed of row and column decoders, multiplexers, memories, and various logic and sequential cells. CIS and IR image sensors are key devices in spacecraft for applications such as earth or space observation, the guidance system in a spacecraft (launcher or satellite). For these reasons, it is necessary to assure the reliability of such systems during the space mission.

Due to the harsh space environment, ROICs are known to be sensitive to single-event effects (SEE), such as single-event transient (SET) and single-event upset (SEU) [4]. One of the main critical failures in the space environment of digital

devices is the loss of functionality of the device, also called single-event functional interrupt (SEFI) [5]. SEFI events are due to an SET or an SEU in a critical function of the device. SETs correspond to a transient change in the state of the node. The criticality of an SET is defined by its intensity, its timing, and its duration. As a function of these characteristics, the SET is able to induce an SEU in the memory function of the device, such as D Flip-Flop (DFF) or static random access memory or an SEFI at the device level. For the space industry, it is necessary to evaluate this risk. Radiation tests with heavy ion or proton beams are used to quantify the SEFI risk on embedded devices or circuits such as ROICs. However, the SEE radiation tests are performed twice: at the beginning of the device/circuit development and at the end. If the results of radiation tests are not acceptable, at this time, it could be critical (technically and financially) to redevelop additional SEFI countermeasures in order to fit with project requirements.

So, the SEFI modeling in ROICs is critical to anticipate the risk due to space radiation. Simulation-based fault injection frameworks allow early evaluation of the system reliability when only the system description and the associate models are available [6]–[11]. Previously, works dedicated to the evaluation of SE have been developed by the means of fault injection at register transfer level using field-programmable gate array (FPGA) and very high description language code. Other approaches are based on the injection of transient errors in flip-flops. However, such work did not take into account other functions of the circuit such as logic cells or clock trees [12]. These approaches are very useful due to their high-speed performances. However, none of these approaches allow linking the injected faults in the studied circuit with the radiation constraint. This makes impossible the quantitative evaluation of the SEFI susceptibility of a given device.

The goal of this paper is to perform the link between a given radiation constraint (heavy ions) and the occurrence of an SEFI. In order to reach this goal, a new SEFI modeling approach is presented and was applied to a studied case: an ROIC designed by Sofradir for their IR image sensor. The SEFI modeling was based on the use of the Monte Radiation tool, MUSCA SEP3 tool [12]–[14] coupled with an new injection platform dedicated to simulate fault injections at multiple system levels: transistor and gate: transient ERROR injection framework for integrated CMOS (TERRIFIC). MUSCA SEP3 will be used to generate a realistic SET database

Manuscript received September 26, 2018; revised October 30, 2018 and November 7, 2018; accepted November 7, 2018. Date of publication November 12, 2018; date of current version January 17, 2019. This work was supported by CNES, French Space Agency, Toulouse, France.

L. Artola and G. Hubert are with ONERA/DPHY, Université de Toulouse, F-31055 Toulouse, France (email: laurent.artola@onera.fr).

S. Ducret and F. Advent are with Sofradir, 38113 Veurey-Voroize, France.

J. Mekki is with CNES-French Space Agency, 31400 Toulouse, France.

Color versions of one or more of the figures in this paper are available online at <http://ieeexplore.ieee.org>.

Digital Object Identifier 10.1109/TNS.2018.2880791

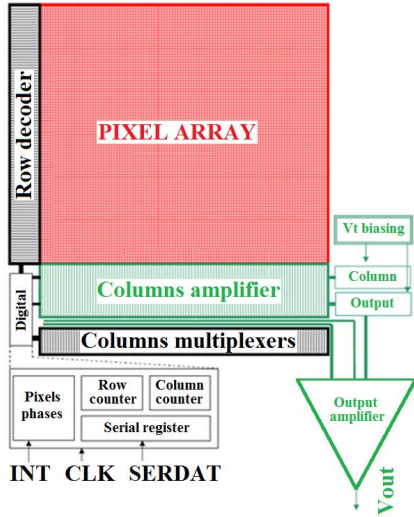


Fig. 1. Overview of the investigated ROIC developed by Sofradir.

(in terms of amplitude and duration) as a function of radiation constraint (energy and location) and device details (technology and designs), while TERRIFIC will allow injecting the SET databases for various configurations (in terms of timing and logical state) in the floating nodes of the device.

This paper is organized as follows. First, the ROIC device will be presented. Second, the experimental results (SEE cross sections) obtained during heavy ion test will be presented. Third, the approach dedicated to the modeling of SEE and especially SEFI will be detailed. Finally, the SEFI estimations will be compared with experimental data and discussed.

II. READOUT INTEGRATED CIRCUIT DEDICATED TO INFRARED IMAGE SENSOR

The readout circuits developed and studied in this paper have been developed by Sofradir in a $0.25\text{-}\mu\text{m}$ bulk technology, with shallow trench isolation [15]. This technology is a mixed technology allowing high voltages on analog parts. This technology allows working at cryogenic temperature: 57 K for this circuit. IR image sensors are cooled down to cryogenic temperature with the aim to reduce the leakage current, also known as the dark current, and to increase its performance.

Fig. 1 presents a global description of the ROIC. The current–voltage conversion was realized by the integration of the input charges on the integrated capacitance. The charges transferred from integration to readout capacitances were then transferred to the amplifiers located in the columns and at the output of the ROIC. The circuit was composed of row and column multiplexers in order to address the pixel arrays.

However, a test transistor was implemented into the direct injection stage to allow the ROIC tests before the hybridization of the detectors. This approach was used for the SEE radiation tests. The ROIC proposes three modes: NORMAL mode, IMAGER mode, and MEMORY mode. The master clock frequency is set at 4 MHz. For confidential reasons, only a brief description of the three modes is presented.

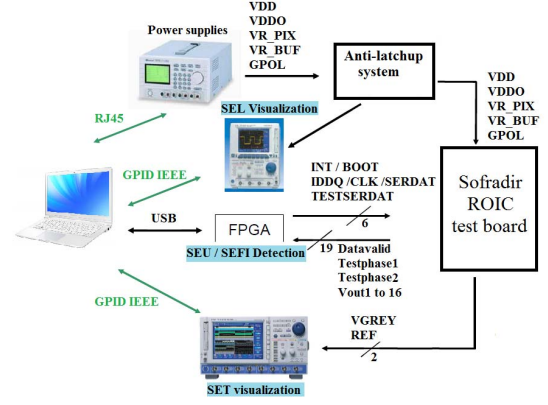


Fig. 2. Experimental setup of SEE detection in ROIC from Sofradir during heavy ion tests.

- *NORMAL Mode*: During this mode, the macropixels are read. The pixel array size is 160×160 . One frame is required to output the whole array.
- *IMAGER Mode*: The aim of this mode is either to perform images with all the subpixels or to detect permanent changes in the subpixel array. This mode will be used to determine the initial subpixel mapping or a new mapping linked to the evolution of the detector during its operational life.
- *MEMORY Mode*: The aim of this mode is to detect state changes in the subpixels memories. These changes are mainly linked to mapping or irradiation issues. The system should store the subpixel mapping to be able to detect the state changes after a MEMORY mode sequence.

In this paper, the modeling of SEFI events was done in the IMAGER mode. Note that in this paper, only the CMOS digital parts of the ROIC were modeled and analyzed.

III. SEFI SENSITIVITY OF SOFRADIR ROIC

A. SEE Irradiation Tests Under Heavy Ions

SEE tests were performed at Université Catholique de Louvain (UCL), Belgium, by the means of the heavy ion facility. The UCL test facility and test beam species were presented in [15]. The principle of the temperature control system used during the heavy ion tests is based on a cooling machine with a cooled finger. The ASIC device is fixed on the top of the cooled finger and directly connected to the vacuum chamber. The complete description of the heavy ion test setup and the temperature control system (at 57 K) was presented in [4] and [5]. The experimental setup is shown in Fig. 2 where the SEFI detection signatures are processed by the FPGA.

Fig. 3 presents the experimental SEE cross sections, for SEU (in black) and for SEFI (in red) of the two ROIC samples (Part1 and Part2) tested in the IMAGER mode under heavy ions. These two samples are issued from the same lot. A strong difference in cross sections is observed for the SEU and the SEFI. The error signature of the observed SEFI corresponds to a change in the mode of operation of the ROIC. This change required an ON/OFF cycle to recover the correct behavior of

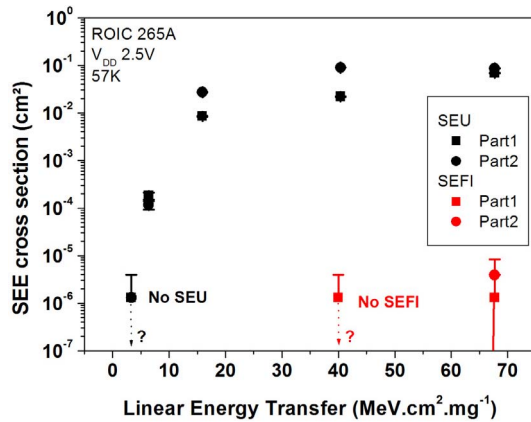


Fig. 3. Experimental SEE cross sections, for SEU (in black) and for SEFI (in red) of the two samples of ROIC under heavy ion beam at 57 K.

the ROIC. Because of project requirements (time and cost reasons) for the SEE qualification of the ROIC, the fluence of each run is about $7.7 \times 10^5 \text{ cm}^{-2}$. This fluence is mandatory by the European Space Components Coordination (ESCC) basic specification No 25 100 for rare SE events [16]. Two samples of ROIC were tested. The SEFI sensitivity of the ROIC is very low. Even if the SEU sensitivity is very well characterized (with very low statistic error bar), it appears that data of SEFI measurements could be completed by simulations.

One of the interests of the modeling of SEFI presented in Section IV will be to provide more data and discuss the reasons of such SEFI robustness. A potential new test plan for a future radiation campaign will be also discussed.

B. Description of the SEFI Modeling Approach

The main principle of this modeling approach is based on the two steps of simulations. Fig. 4 presents the global framework of the SEFI modeling approach.

The Monte Carlo (MC) radiation tool, MUSCA SEP3, was used [12], [14], [15]. This tool has been developed at ONERA since 2008. As mentioned, the tool uses a MC approach coupled in a sequential modeling of all the physical and electrical processes. The following steps are considered: 1) the modeling of the radiation constraint; 2) the transport mechanisms of radiation particles (in this work, heavy ions) through the layer stack (back end of line); 3) the generation of electron-hole pairs in the silicon; 4) the mechanisms of charges transport and collection; and 5) the circuit feedback.

The modeling of the radiation environment is based on several sources of input data (from engineering models, and physical models). These models are provided by ONERA's internal research group which is considered as a worldwide reference [17].

The modeling of transport mechanisms of radiation particles through the overlayers is based on databases from GEANT4 (for nuclear reactions) and stopping and range of ions in matter (for ionization mechanism). The interest of using databases is the time-consuming gain in comparison with full direct simulations.

The modeling transport and collection of free carriers in the silicon are performed by the means of 3-D analytical

models in order to take into account the following mechanisms: ambipolar diffusion, dynamic collection, multicollection bipolar amplification, recombination, bias dependence, and temperature dependence. It is important to highlight that all the physical and electrical models used for the transport and collection of charge in the semiconductor take into account the impact of the temperature, down to 50 K. Specific models occurring at cryogenic temperature such as incomplete ionization of dopant atom of the substrate, shallow level impact ionization, and band-to-band narrowing were considered to take into account the decrease in the mobility of carriers below 150 K as revealed by recent works for radiation effect applications [18], [19].

The modeling of the front end of line is based on a description (dimensions and locations) of drain and source implants of each nMOS and pMOS transistors. This information was extracted by a graphic database system extractor from the design file provided by Sofradir.

This simulation framework allows for obtaining an SET database. The communication link between MUSCA SEP3 and the Specter simulator was done by the means of a new simulation framework called TERRIFIC. This injection tool allows for performing electrical SET injections at various levels: 1) transistor level or 2) gate level.

At transistor level, the injections are performed using the SET database generated by MUSCA SEP3 as done in [14] and [15]. The cryogenic transistor models were developed and validated by Sofradir using experimental data from $I-V$ measurements. These simulations allowed estimating the SET and SEU cross sections of a set of basic digital cells used in the ROIC. After an analysis of the layout of the ROIC, three main families of standard cells were selected: logic cells, DFF, and clock buffers. This selection is based on a preliminary fault injection simulation at gate level of the ROIC. These cell families correspond to the majority of the area of the digital part of the ROIC. It was revealed that the standard cells of the process design kit (PDK) used by Sofradir for their ROIC have very similar SET/SEU cross sections for various designs in each digital function, especially at cryogenic temperatures (57 K) [4], [20]. According to these works, a hypothesis of a variation of $\pm 25\%$ of SET/SEU cross section would be considered for each main family of standard cells. The $\pm 25\%$ correspond to an engineering estimate of the variability of the SEE sensitivity of the standard cells based on experimental measurements and simulations performed in [20]. MUSCA SEP3 simulations were performed for one reference of each of the selected main families. The respective SEE cross sections will be presented and discussed in the next section.

At gate level, TERRIFIC performs fault injection simulations based on the SEE evaluation of SET injections (issued from MUSCA SEP3). The characteristics of these SETs correspond to the worst cases in terms of amplitude and duration.

At the same time, automated fault injection simulations were performed on the digital modules of the ROIC using the TERRIFIC tool developed in SKILL [21]. The fault injection was done at the gate level on each floating node of the circuitry using the Spectre simulator. For SEEs (expected

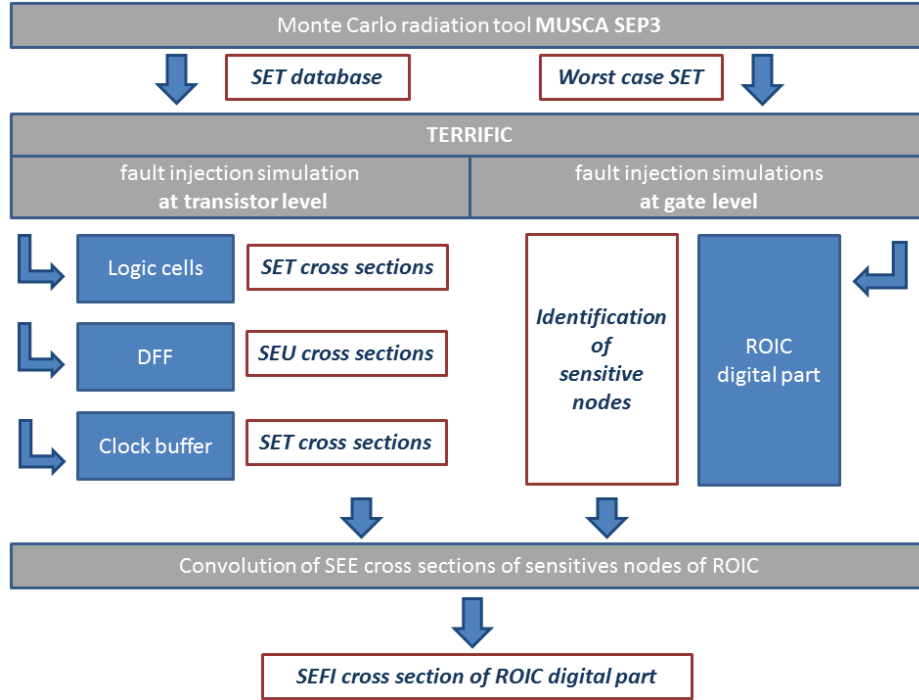


Fig. 4. General framework of SEFI modeling in the digital part of the ROIC based on MUSCA SEP3 and TERRIFIC. Gray: simulations and calculation steps. Blue: simulation targets (gate and device). Red rectangles: inputs/outputs of simulations and calculations.

for single-event latchup), the floating nodes are the only nodes whose the electrical potential can be disturbed by a transient current. The other nodes, i.e., connected to the ground, mitigate the transient currents from the circuit. Injections of current pulses were simulated on clocked signals, while injections of voltage pulses were simulated on the other floating nodes. This allowed for not disturbing the nominal bias of the ROIC before the fault injection. The simulations allowed identifying the sensitive nodes and the associated standard cells, which could induce an SEFI in the digital part of the ROIC.

The identification of sensitive nodes and the SEE cross section of logic cells, DFF, and clock buffers were convolved to determine the SEFI cross section of the ROIC. The calculation of the SEFI cross section corresponds to the sum of SEU/SEU cross sections obtained for the gates which are connected with the identified sensitive nodes.

IV. DISCUSSION

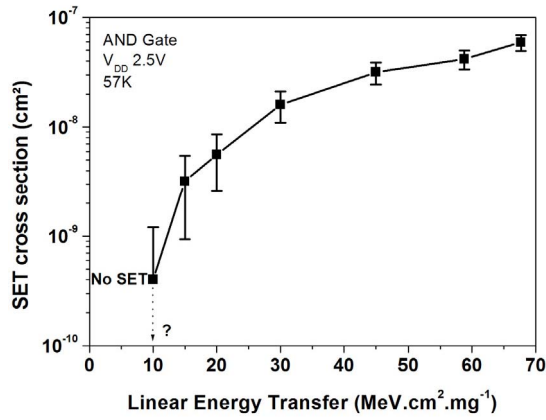
Fig. 5 shows the simulations of SEE (SET and SEU) cross sections of the selected reference for each cell family: logic, DFF, and clock buffers. The selection of the evaluated cell for each family was done randomly. However, as mentioned previously, due to the very limited variability of the SEE sensitivity of the standard cells for each family, it is considered that a sensitivity envelope of $\pm 25\%$ around the presented SET/SEU cross section will be considered for the logic/DFF/clock buffer cells of the PDK.

The results of MUSCA SEP3 simulations coupled with TERRIFIC runs were obtained for a simulated fluence of

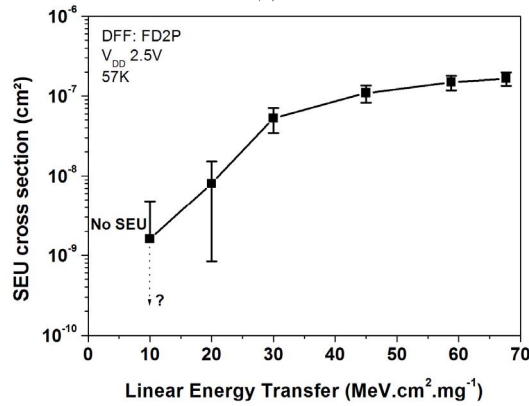
1×10^8 up to $1 \times 10^9 \text{ cm}^{-2}$ regarding the investigated cell. The error bars correspond to two times of the standard deviation (97% of confidence). Fig. 5 (a) presents the SET cross section of a reference of AND gates as a function of linear energy transfer (LET) of heavy ions simulated at 57 K. As expected for the SET, the saturation of the cross section is not well observed. The phenomenon is due to the low drive current for this design of the AND gate [20].

Fig. 5(b) presents the SEU cross section of a reference of DFF as a function of heavy ion LETs simulated at 57 K. The LET threshold is the same as the AND gate (i.e., $10 \text{ MeV}\cdot\text{cm}^2\cdot\text{mg}^{-1}$) illustrated in Fig. 5(a)–5(c) by a dashed arrow and a question mark. Fig. 5(c) presents the SET cross section of a reference of clock buffer as a function of heavy ion LETs. No event was observed during the simulations at 57 K (in black). In order to evaluate if the cell is totally immune to SET, an increase in the temperature was simulated. An increase in temperature is known to lead to an increase in the SET duration [22]. This point is in good correlation with previous works which highlighted that if a cryogenic temperature dependence of SEE occurrence is observed, the worst case must be not at cryogenic temperature but at room temperature [19]. The simulations highlight the potential SET sensitivity of the clock buffer at 300 K (in red). However, for the ROIC point of view, the contribution of clock buffers to the SEFI occurrence is very limited ($\sim 10\%$).

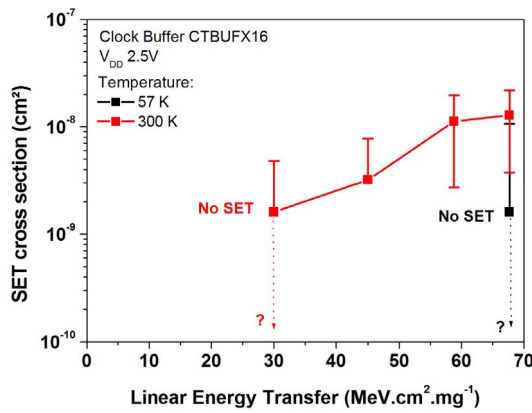
As mentioned in Section III-B, these SEE cross sections were convolved with the identified sensitive nodes of the ROIC (thanks to the fault injection simulation). The calculation of the SEFI cross section corresponds to the sum of SEU/SEU cross sections obtained for the gates



(a)



(b)



(c)

Fig. 5. Simulations of SEU and SET cross sections of: (a) AND gate, (b) DFF, and (c) clock buffer.

which are connected the identified sensitive nodes. This final step allowed calculating the SEFI sensitivity of the ROIC.

Fig. 6 presents the comparison of experimental (red symbols) and simulation (black symbols) data of the SEFI cross section of the ROIC as a function of LET of heavy ions at 57 K. The error bars correspond to two times of the standard deviation (97% of confidence). The simulations are in good correlation with the experimental data and confirm the strong robustness of the ROIC against SEFI. However, the wide error bars in the experimental data needed to be validated. As mentioned, because of project requirements (time and cost reasons) for the SEE qualification of the ROIC, the fluence of

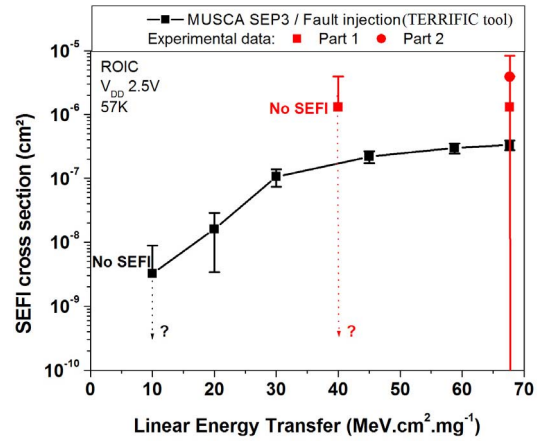


Fig. 6. Comparison of experimental (red symbols) and simulation (black symbols) of the SEFI cross section of ROIC as a function of LET of heavy ions at 57 K.

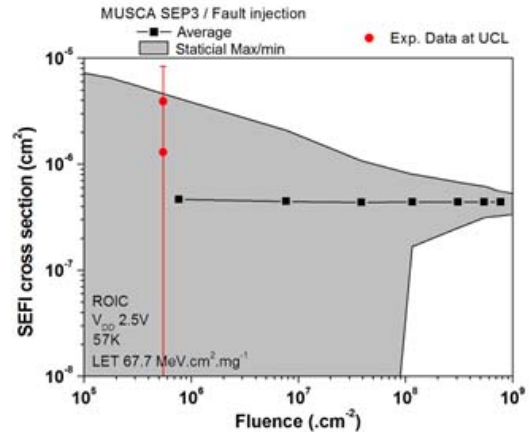


Fig. 7. Comparison of experimental data (in red) and MC simulation of the SEFI cross section as a function of deposited fluence of $67.6 \text{ MeV}\cdot\text{cm}^2\cdot\text{mg}^{-1}$ heavy ions.

each irradiation run is about $7.7 \times 10^5 \text{ cm}^{-2}$. This fluence is mandatory by the ESCC basic specification No 25 100 for SEE [16]. For this reason, SEU and SEFI were measured in the same time for each irradiation run. Even if the SEU sensitivity was very well characterized (with very low statistic error bar), it appears that data of SEFI measurements are weak and could be completed by dedicated simulations as a function of fluence.

Fig. 7 presents the calculated SEFI cross section by MC simulation as a function of fluence. It integrates the evolution of the statistical minimum/maximum error corresponding to two times of the standard deviation (97% of confidence). The simulation results show a similar SEFI sensitivity (between 1×10^{-6} and $4 \times 10^{-6} \text{ cm}^2$) obtained for the same fluence used during experimental tests ($7.7 \times 10^5 \text{ cm}^{-2}$). The simulation results confirmed the weak deposited fluence during experimental data for a relevant quantitative evaluation of the SEFI sensitivity of the ROIC. Considering the simulation results a relevant fluence would be around 1×10^8 and $5 \times 10^9 \text{ cm}^{-2}$.

In the future projects, the radiation test plan of ROICs developed by Sofradir will be updated. In addition to the standard specification from ESCC (for SEU tests), a dedicated

run for SEFI measurement could be performed with high fluence levels. This specific SEFI test plan will be developed regarding preliminary simulations of this new SEFI modeling approach. In this case of the robust IR detector, a relevant fluence should reach $1 \times 10^8 \text{ cm}^{-2}$ for the highest LET. Even if such increase in fluence is not representative of a given space mission for earth orbits, it would improve the understanding of SEFI in complete digital systems under a radiation constraint.

V. CONCLUSION

This paper presents a modeling approach of SEFI which takes into account all the physical and electrical processes from the radiation particle down to the event at the system level. This paper was focused on the evaluation of SEFI sensitivity by experimental and simulation analyses of an ROIC designed by Sofradir for their IR image sensors. Relevant correlations between simulation and experimental results of SEFI cross sections for heavy ions were presented and discussed. The relevance of the SEFI estimation is allowed by the complete description of the device: layout, size, and technology. The simulation results confirmed the strong SEFI robustness of the ROIC at 57 K.

The SEFI modeling approach has presented promising applications for radiation hardness assurance. Due to the need to get as an input the complete description of the device (layout and technology), this approach is relevant and useful for designers for the preparation of future radiation tests. For rare events such as SEFI, it allows obtaining a first sensitive level of the device before radiation tests and defining potentially higher fluence than the regular radiation standards with the aim to reduce error bars if needed. Even if such increase in fluence during radiation test is not representative of a given space mission for earth orbits, it would improve the understanding of SEFI mechanisms in complete digital systems under a radiation constraint.

By definition, the SEFI evaluation defines the operability rate of a given system. Other promising perspectives of such SEFI modeling approach will be the operational evaluation of an embedded system used in a given space integration platform for various orbits.

REFERENCES

- [1] G. R. Hopkinson, "Radiation effects in CMOS active pixel sensor," *IEEE Trans. Nucl. Sci.*, vol. 47, no. 6, pp. 2480–2484, Dec. 2000.
- [2] D. Falguere *et al.*, "In-flight observations of the radiation environment and its effects on devices in the SAC-C polar orbit," *IEEE Trans. Nucl. Sci.*, vol. 49, no. 6, pp. 2782–2887, Dec. 2002.
- [3] P. Caron *et al.*, "Physical mechanisms inducing electron single-event upset," *IEEE Trans. Nucl. Sci.*, vol. 65, no. 8, pp. 1759–1767, Aug. 2018.
- [4] A. Al Youssef *et al.*, "Single-event transients in readout circuitries at low temperature down to 50 K," *IEEE Trans. Nucl. Sci.*, vol. 65, no. 1, pp. 119–125, Jan. 2018.
- [5] L. Artola *et al.*, "Single event transient and functional interrupt in readout integrated circuit of infrared image sensors at low temperatures," in *Proc. IEEE Radiat. Effects Data Workshop*, Jul. 2017, pp. 1–5.
- [6] R. Leveugle, "Fault injection in VHDL descriptions and emulation," in *Proc. IEEE Int. Symp. Defect Fault Tolerance VLSI Syst.*, Oct. 2000, pp. 414–419.
- [7] P. S. Magnusson *et al.*, "Simics: A full system simulation platform," *IEEE Comput.*, vol. 35, no. 2, pp. 50–58, Feb. 2002.
- [8] G. C. Cardarilli, F. Kaddour, A. Leandri, M. Ottavi, S. Pontarelli, and R. Velazco, "Bit flip injection in processor-based architectures: A case study," in *Proc. 8th IEEE Int. On-Line Test. Workshop (IOLTW)*, Jul. 2002, pp. 117–127.
- [9] N. Binkert *et al.*, "The gem5 simulator," *ACM SIGARCH Comput. Archit. News*, vol. 39, no. 2, pp. 1–7, 2011.
- [10] J. Xu and P. Xu, "The research of memory fault simulation and fault injection method for BIT software test," in *Proc. 2nd Int. Conf. Instrum. Meas., Comput., Commun. Control*, Dec. 2012, pp. 718–722.
- [11] F. de Aguiar Geissler, F. L. Kastensmidt, and J. E. P. Souza, "Soft error injection methodology based on QEMU software platform," in *Proc. IEEE Latin Amer. Test Workshop (LATW)*, Mar. 2014, pp. 1–5.
- [12] H. Cho, S. Mirkhani, C.-Y. Cher, J. A. Abraham, and S. Mitra, "Quantitative evaluation of soft error injection techniques for robust system design," in *Proc. 50th IEEE Design Autom. Conf. (DAC)*, May/June. 2013, pp. 1–10.
- [13] G. Hubert, S. Duzellier, C. Inguibert, C. Boatella-Polo, F. Bezerra, and R. Ecoffet, "Operational SER calculations on the SAC-C orbit using the multi-scales single event phenomena predictive platform (MUSCASP³)," *IEEE Trans. Nucl. Sci.*, vol. 56, no. 6, pp. 3032–3042, Dec. 2009.
- [14] G. Hubert and L. Artola, "Single-event transient modeling in a 65-nm bulk CMOS technology based on multi-physical approach and electrical simulations," *IEEE Trans. Nucl. Sci.*, vol. 60, no. 6, pp. 4421–4429, Dec. 2013.
- [15] L. Artola *et al.*, "Single event upset sensitivity of D-flip flop of infrared image sensors for low temperature applications down to 77 K," *IEEE Trans. Nucl. Sci.*, vol. 62, no. 6, pp. 2979–2987, Dec. 2015.
- [16] *ESA Radiation Standards and Guidelines*. Accessed: Oct. 30, 2018. [Online]. Available: <https://escies.org>
- [17] S. Bourdarie and M. Xapsos, "The near-earth space radiation environment," *IEEE Trans. Nucl. Sci.*, vol. 55, no. 4, pp. 1810–1832, Aug. 2008.
- [18] A. Al Youssef, L. Artola, S. Ducret, G. Hubert, and F. Perrier, "Investigation of electrical latchup and SEL mechanisms at low temperature for applications down to 50 K," *IEEE Trans. Nucl. Sci.*, vol. 64, no. 8, pp. 2089–2097, Aug. 2017.
- [19] L. Artola *et al.*, "Update of single event effects radiation hardness assurance of readout integrated circuit of infrared image sensors at cryogenic temperature," *Sensors*, vol. 18, no. 7, pp. 2338–2350, Jul. 2018.
- [20] L. Artola, G. Hubert, S. Ducret, J. Mekki, A. Al Youssef, and N. Ricard, "Impact of D-flip-flop architectures and designs on single-event upset induced by heavy ions," *IEEE Trans. Nucl. Sci.*, vol. 65, no. 8, pp. 1776–1782, Aug. 2018.
- [21] T. J. Barnes, "SKILL: A CAD system extension language," in *Proc. IEEE 27th ACM/IEEE Design Autom. Conf.*, Jun. 1990, pp. 266–271.
- [22] L. Artola and G. Hubert, "Modeling of elevated temperatures impact on single event transient in advanced CMOS logics beyond the 65-nm technological node," *IEEE Trans. Nucl. Sci.*, vol. 61, no. 4, pp. 1610–1617, Aug. 2014.